AGU PUBLICATIONS

Geophysical Research Letters

RESEARCH LETTER

10.1002/2015GL065022

Key Points:
- The relation between impact-generated porosity and crater size is quantified
- Impacts into highly porous targets result in positive gravity anomalies
- The cratering record of the oldest lunar surfaces is preserved in the subsurface

Supporting Information:
- Supporting Information S1

Correspondence to:
J. M. Soderblom,
jms4@mit.edu

Citation:
Soderblom, J. M., et al. (2015), The fractured Moon: Production and saturation of porosity in the lunar highlands from impact cratering, *Geophys. Res. Lett.*, *42*, 6939–6944, doi:10.1002/2015GL065022.

Received 21 JUN 2015
Accepted 6 AUG 2015
Accepted article online 11 AUG 2015
Published online 10 SEP 2015

The fractured Moon: Production and saturation of porosity in the lunar highlands from impact cratering

Jason M. Soderblom[1], Alexander J. Evans[2], Brandon C. Johnson[1], H. Jay Melosh[3], Katarina Miljković[1,4], Roger J. Phillips[5], Jeffrey C. Andrews-Hanna[6], Carver J. Bierson[7], James W. Head III[8], Colleen Milbury[3], Gregory A. Neumann[9], Francis Nimmo[7], David E. Smith[1], Sean C. Solomon[2,10], Michael M. Sori[11], Mark A. Wieczorek[12], and Maria T. Zuber[1]

[1]Department of Earth, Atmospheric and Planetary Sciences, Massachusetts Institute of Technology, Cambridge, Massachusetts, USA, [2]Lamont-Doherty Earth Observatory, Columbia University, Palisades, New York, USA, [3]Department of Earth, Atmospheric, and Planetary Sciences, Purdue University, West Lafayette, Indiana, USA, [4]Now at Department of Applied Geology, Curtin University, Perth, Western Australia, Australia, [5]Planetary Science Directorate, Southwest Research Institute, Boulder, Colorado, USA, [6]Department of Geophysics and Center for Space Resources, Colorado School of Mines, Golden, Colorado, USA, [7]Department of Earth and Planetary Sciences, University of California, Santa Cruz, California, USA, [8]Department of Earth, Environmental and Planetary Sciences, Brown University, Providence, Rhode Island, USA, [9]NASA Goddard Space Flight Center, Greenbelt, Maryland, USA, [10]Department of Terrestrial Magnetism, Carnegie Institution of Washington, Washington, District of Columbia, USA, [11]Lunar and Planetary Laboratory, University of Arizona, Tucson, Arizona, USA, [12]Institut de Physique du Globe de Paris, Sorbonne Paris Cité, Université Paris Diderot, Paris, France

Abstract We have analyzed the Bouguer anomaly (BA) of ~1200 complex craters in the lunar highlands from Gravity Recovery and Interior Laboratory observations. The BA of these craters is generally negative, though positive BA values are observed, particularly for smaller craters. Crater BA values scale inversely with crater diameter, quantifying how larger impacts produce more extensive fracturing and dilatant bulking. The Bouguer anomaly of craters larger than 93^{+47}_{-19} km in diameter is independent of crater size, indicating that there is a limiting depth to impact-generated porosity, presumably from pore collapse associated with either overburden pressure or viscous flow. Impact-generated porosity of the bulk lunar crust is likely in a state of equilibrium for craters smaller than ~30 km in diameter, consistent with an ~8 km thick lunar megaregolith, whereas the gravity signature of larger craters is still preserved and provides new insight into the cratering record of even the oldest lunar surfaces.

1. Introduction

The high porosity of the lunar crust extends to at least 10–25 km in depth [*Besserer et al.*, 2014] and perhaps into the Moon's upper mantle [*Wieczorek et al.*, 2013]. Because the lunar highland crust has undergone little modification by processes other than impacts, it provides an ideal setting to investigate porosity in the crusts of terrestrial planetary bodies and serves as an analog to the crusts of Archean Earth and pre-Noachian Mars. Porosity affects permeability, surface area, and thermal conductivity of crustal and upper mantle rocks. Improved understanding of the spatial and temporal evolution of crustal porosity will provide insight into the chemical and mechanical reaction rates that drive many geological and ecological processes [e.g., *Navarre-Sitchler and Brantley*, 2007] and the thermal and chemical evolution [e.g., *Warren and Rasmussen*, 1987] of planetary bodies.

Although impact cratering is likely to have been the primary mechanism responsible for generating porosity in primordial planetary lithospheres, the relevant processes are poorly constrained. Impacts are believed to increase near-surface porosity by brecciation interior and exterior to the crater and porosity at depth by fracturing and dilatancy [*Pilkington and Grieve*, 1992; *Alejano and Alonso*, 2005; *Collins*, 2014]. Impacts are also thought to decrease crustal porosity through localized heating and compaction of the target rock [*Melosh*, 1989; *Milbury et al.*, 2015], but there have been no observations capable of constraining these effects at the scales of planetary impact craters. Previous investigations have been limited to gravity and seismic observations of terrestrial craters (which have been substantially modified by erosion), with no more than half a dozen examined in detail [*Innes*, 1961; *Pohl et al.*, 1977; *Pilkington and Grieve*, 1992; *Henkel et al.*, 2010], and low-resolution gravity profiles of ~100 lunar craters [*Dvorak and Phillips*, 1977; *Sugano and Heki*, 2004].

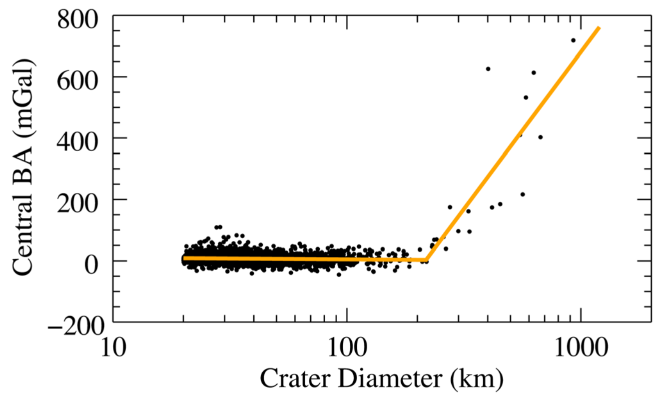

Figure 1. $BA_{central}$ versus *D* for craters formed in the lunar highlands. $BA_{central}$ is sensitive to excess mass beneath the central region of the crater, from which we infer the presence of uplifted mantle material. These data statistically support a break in slope at a $D > 218 \pm 17$ km (indicated by the best fit two-slope model in orange).

Here we present the first comprehensive analysis of impact-generated fracturing of an ancient planetary surface as a critical first step in understanding these processes.

2. Gravity Data

The Gravity Recovery and Interior Laboratory (GRAIL) mission [*Zuber et al.*, 2013] has afforded unprecedented insight into the structure of the lithosphere of the Moon. From GRAIL data we may infer a porosity contrast between crustal material modified by the formation of an impact crater and the surrounding crust, under the assumption that the grain density of both materials is similar. For this work we used the JGGRAIL_900C9A gravity field [*Konopliv et al.*, 2014] assembled at the Jet Propulsion Laboratory from GRAIL Primary and Extended Mission data [*Zuber et al.*, 2013] and expanded in spherical harmonics to degree and order 900. To this field, we applied a Bouguer correction to remove the gravitational contribution of surface topography. Our Bouguer correction used the principal-axis-referenced solution for topography from the Lunar Orbiter Laser Altimeter (LOLA) [*Smith et al.*, 2010] and a uniform bulk crustal density of 2560 kg m^{-3} [*Wieczorek et al.*, 2013], though our results hold for variations in the mean bulk density consistent with current uncertainties (see supporting information). We then filtered this field to include data between degree and order 7 and degree and order 580, with a cosine taper applied between degrees 550 and 580. This maximum degree corresponds to a half-wavelength of 9 km. This Bouguer gravity anomaly field is shown in Figure S1 in the supporting information.

3. Lunar Highland Impact Craters

The craters selected for our study are from a catalog of ~5200 craters [*Head et al.*, 2010] identified from LOLA topography [*Smith et al.*, 2010]. We limited our investigation to a single morphological class of impact structures: complex craters (i.e., craters with terraced walls, a generally flat floor, and a central peak or peak ring). We set a lower diameter limit of 27 km, on the basis of the maximum observed size of simple (bowl shaped) craters on the Moon [*Pike*, 1988]. As our focus is on impact-generated porosity of the highland megaregolith, we excluded craters that are so large as to have interacted with the mantle during their formation. During the formation of a sufficiently large impact structure, mantle material is uplifted during collapse of the transient crater. The greater density of mantle relative to crustal material results in a central excess mass [*Wieczorek and Phillips*, 1999; *Melosh et al.*, 2013; *Miljković et al.*, 2013; *Freed et al.*, 2014], which dominates the structure's gravity signature, limiting our ability to infer information about porosity. We therefore set an upper diameter limit on the basis of the onset, with increasing diameter, of mantle uplift beneath the impact feature.

We used the gravity signature of this uplifted mantle to identify these structures and to exclude them from our analysis. We define the central Bouguer anomaly ($BA_{central}$) of an impact structure as the area-weighted mean Bouguer anomaly from the crater center to a radial distance of 0.2 *R* less the area-weighted mean Bouguer anomaly within an annulus that extends radially from 0.5 to 1.0 *R*, where *R* is the radius of the crater rim crest. In Figure 1, we plot $BA_{central}$ as determined from GRAIL observations of highland impact structures, as a function of *D*, the diameter of the crater rim crest. We fit these data with a log linear two-slope model and applied Bayesian statistics, following the approach of *Main et al.* [1999] (see supporting information) to determine whether the data support a break in slope that would indicate the detection of uplifted mantle material. We determined that the onset of mantle uplift for impacts into the lunar highlands occurs at a diameter of 218 ± 17 km (all errors are 95% confidence limits; see supporting information for additional details).

On the basis of these results, we set 201 km (the lower uncertainty bound on onset diameter for mantle uplift in the highlands) as the uppermost diameter for the craters we used to investigate impact-generated

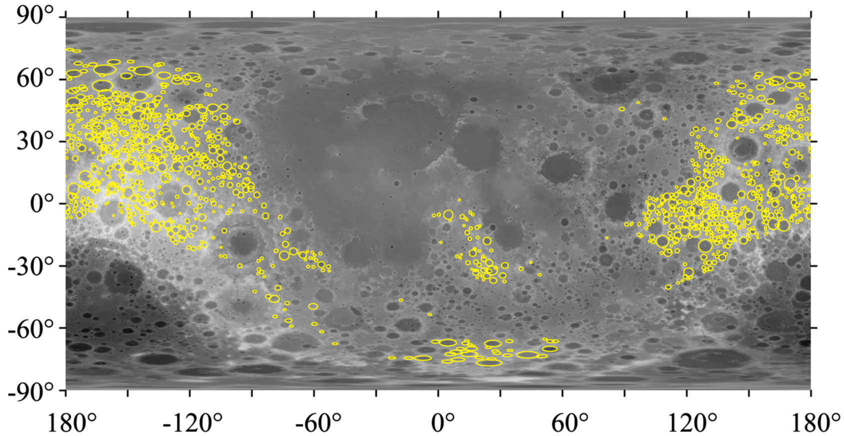

Figure 2. Outlines (in yellow) of the 1185 complex lunar highland craters used for this work. The background image is a gray-scale LOLA topography map (cylindrical projection) that is centered on the nearside.

porosity. We also excluded craters on the rim of South Pole-Aitken basin, on the grounds that the structure of the crust beneath these craters differs from that beneath typical highland craters [*Phillips et al*., 2015]. We were left with 1185 highland craters for further analysis of crustal porosity. The locations of these craters are shown in Figure 2.

4. Gravity Signatures of Impact Craters

The gravity anomalies associated with impact-generated porosity of terrestrial craters are observed to extend to, or in some cases slightly beyond, the crater rim crest [*Pilkington and Grieve*, 1992]. To constrain impact-generated porosity for each of the craters in our study, we calculated a residual Bouguer anomaly ($BA_{residual}$), which we define as the area-weighted mean Bouguer anomaly interior to the crater rim less the mean Bouguer anomaly within a background annulus that extends radially from the outer flank of the rim [*Pike*, 1977] to a distance of 2 R from the crater center. Subtracting the background gravity anomaly isolates the gravity signature of the crater itself from regional variations in the gravity field, such as those introduced by large-scale variations in crustal density or thickness, and reduces bias in the data introduced by differences between the reference elevation of the gravity field and the elevations of the craters.

The background annulus includes the continuous ejecta deposit and, therefore, has the potential for biasing our results if there are measurable systematic trends in the Bouguer signature of crater ejecta deposits as a function of crater size. Selecting an annulus with an inner diameter farther from the crater would reduce this potential bias but would yield background measurements that are less precise and therefore noisier (i.e., our results would likely be more accurate but at the cost of precision). To determine whether our data are biased by our choice of a background region, we plotted the mean Bouguer anomaly measured in the background annulus as a function of crater diameter (Figure S2 in the supporting information). No relation between D and the background BA measurement is observed. As a confirmation, we reanalyzed our data, as described below, with larger background annuli (in which the background annulus extended from 2.0 D to 2.5 D and 2.4 D to 3.0 D), and our results were unchanged.

5. Results

We examine the relation between $BA_{residual}$ and crater size in Figure 3. The $BA_{residual}$ value of highland craters correlates inversely with D, up to a diameter of ~100 km. $BA_{residual}$ is negative on average, implying that porosity beneath complex craters is generally higher than in the surrounding crust. Considerable variability, however, on the order of ±25 mGal about the mean, is observed. Some craters, in fact, exhibit positive $BA_{residual}$ values, suggesting that the bulk density of the underlying material is actually higher than that of the surrounding terrain. An apparent change in the relation between D and $BA_{residual}$ is observed at a crater diameter of ~100 km. We fit these data to a two-slope model (see supporting information for details) and find that they support a statistically significant break in slope at a D of 93^{+47}_{-19} km.

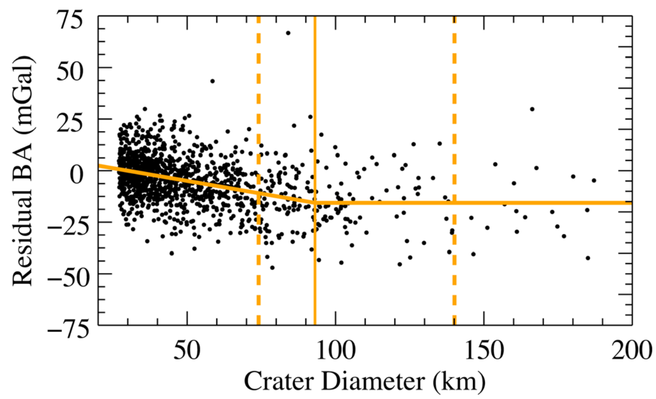

Figure 3. $BA_{residual}$ versus D for the set of 1185 complex lunar highlands craters analyzed in this study. The data support a statistically significant break in slope at a diameter of 93^{+47}_{-19} km, which we attribute to a reduction in impact-generated porosity at depths greater than a limiting value. Dashed lines indicate the 95% confidence limits to this transition diameter.

We interpret the relation between $BA_{residual}$ and D for craters with $D < 93$ km to imply that larger impacts in this crater diameter range result in more extensive fracturing and dilatant bulking. Thus, the amount of impact-generated pore space is expected to depend on parameter(s) of the impact (e.g., size, velocity, and/or angle). The $BA_{residual}$ value of craters with $D > 93$ km, in contrast, appears to be independent of D, implying that pore collapse from either viscous flow at high temperature [*Wieczorek et al.*, 2013] or overburden pressure [*Collins*, 2014] has acted to remove, or prevented the formation of, impact-generated porosity at depths greater than some limiting value. We propose that this limiting depth corresponds to the discontinuity observed in the seismic velocity profile of the lunar crust at a depth of ~20–25 km [*Toksöz et al.*, 1974]. Terrestrial craters exhibit similar limits in Bouguer anomaly for craters larger than ~20–30 km diameter, a result interpreted as evidence that lithostatic pressure closes pore space at depths greater than ~8 km on Earth [*Pilkington and Grieve*, 1992].

The observed $BA_{residual}$ value is likely to depend on the characteristics of the impact and target region (e.g., preimpact porosity, strength, density, and thermal gradient). The variability observed in $BA_{residual}$ at a given D likely reflects spatial and temporal variations in these properties. Postimpact modification (e.g., brecciation and infilling from subsequent impacts and magmatic intrusions) might also be important. Although impact parameters are weakly constrained, we can investigate the role of preimpact crustal properties by plotting $BA_{residual}$ against the porosity of the surrounding crust, measured as the area-weighted mean within the background annulus (Figure 4) of the porosity as derived from GRAIL data [*Wieczorek et al.*, 2013]. We find that positive values of $BA_{residual}$ correlate with high porosity in the surrounding crust. This result supports the conclusions derived from recent modeling that impacts can reduce porosity if the preimpact target material is sufficiently porous [*Scott and Wilson*, 2005; *Milbury et al.*, 2015]. The implication is that in the absence of other major processes (e.g., magmatism and large-scale impacts), and averaged over appropriate horizontal scales, the processes of porosity generation and compaction by impact will tend toward an equilibrium porosity that is, on average, uniform over large regions but may exhibit local fluctuations associated with freshly formed craters. The scatter about the best fit relation in Figure 4, however, indicates that regional variations in porosity are unable to account for all of the variability in $BA_{residual}$. Additional modeling to explore the effects of impact and target properties on the formation of impact-generated porosity, as well

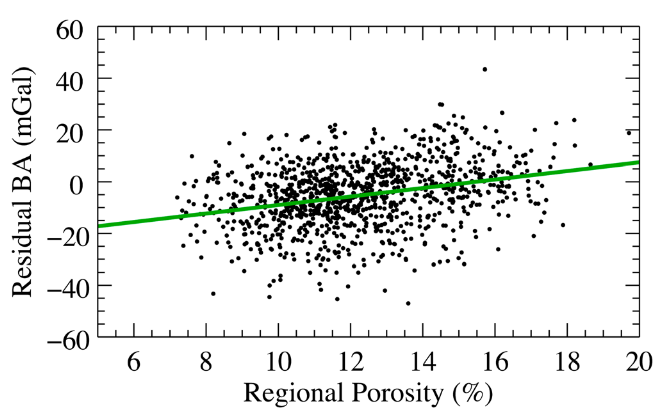

Figure 4. $BA_{residual}$ versus the bulk porosity of the surrounding crust, derived from GRAIL observations and a grain density inferred from remote sensing [*Wieczorek et al.*, 2013], for the craters shown in Figure 2. A direct relation between crater Bouguer anomaly and regional crustal porosity is observed (green line, with a slope of 1.6 ± 0.3 mGal per percent change in porosity), which indicates that impact-generated porosity depends on the porosity of the target material prior to impact. The best fit trend has a zero $BA_{residual}$ value at a regional crustal porosity of 15 ± 1%.

as more detailed geological, geochemical, and geophysical analyses of individual craters, may provide additional insight.

We predict that craters that are in a state of equilibrium in porosity will have $BA_{residual}$ values near zero and will be independent of *D*. The generally negative Bouguer anomalies of complex impact craters in the lunar highlands (Figure 3) indicate that the highlands have not reached a state of saturation of impact-generated porosity for craters larger than ~30 km in diameter. If the impact-generated porosity zone extends to depths similar to the transient crater depth (approximately one-fourth to one-third the final crater diameter), the results here suggest that the porosity of lunar highland crust is in an approximate steady state down to no more than ~8 km depth, a result consistent with estimates of the thickness of the lunar megaregolith [*Hörz et al*., 1991]. As is demonstrated in Figure S3 in the supporting information, however, the choice of crustal density in the Bouguer correction can bias the $BA_{residual}$ values, so the precise diameter at which equilibrium is reached is uncertain.

The surface of the lunar highlands is thought to be in a state of areal saturation with respect to impact craters [*Head et al*., 2010], whereby, on average, each new impact crater destroys a preexisting crater of comparable size [*Hartmann*, 1980; *Richardson*, 2009]. As a consequence, the size-frequency distribution of craters in the lunar highlands does not accurately reflect the local age of the highland crust. The subsurface structure of the highlands, however, is not in a state of porosity equilibrium and preserves a more complete record of the region's cumulative cratering history. Advances in crater modeling should allow the identification of the oldest areas of highland crust and possibly also permit the recovery of the cumulative cratering record of the highlands, including the record prior to the late heavy bombardment [*Minton et al*., 2015; *Strom et al*., 2015].

Acknowledgments
We thank all those involved with the development and operations of the GRAIL spacecraft and the collection and reduction of the GRAIL data. We also thank Sai Ravela (MIT) for his guidance with the statistical analyses used in this paper. Gareth Collins and Boris Ivanov provided constructive reviews that helped to improve this manuscript. This work was funded by the GRAIL mission, which is supported by the NASA Discovery Program, and is performed under contract to the Massachusetts Institute of Technology and the Jet Propulsion Laboratory, California Institute of Technology. Data used in this paper are archived in the Geophysics Node of the Planetary Data System.

The Editor thanks Gareth Collins and Boris Ivanov for their assistance in evaluating this paper.

References

Alejano, L. R., and E. Alonso (2005), Considerations of the dilatancy angle in rocks and rock masses, *Int. J. Rock Mech. Min. Sci.*, *42*, 481–507, doi:10.1016/j.ijrmms.2005.01.003.

Besserer, J., F. Nimmo, M. A. Wieczorek, R. C. Weber, W. S. Kiefer, P. J. McGovern, J. C. Andrews-Hanna, D. E. Smith, and M. T. Zuber (2014), GRAIL gravity constraints on the vertical and lateral density structure of the lunar crust, *Geophys. Res. Lett.*, *41*, 5771–5777, doi:10.1002/2014GL060240.

Collins, G. S. (2014), Numerical simulations of impact crater formation with dilatancy, *J. Geophys. Res. Planets*, *119*, 2600–2619, doi:10.1002/2014JE004708.

Dvorak, J., and R. J. Phillips (1977), The nature of the gravity anomalies associated with large young lunar craters, *Geophys. Res. Lett.*, *4*, 380–382, doi:10.1029/GL004i009p00380.

Freed, A. M., B. C. Johnson, D. M. Blair, H. J. Melosh, G. A. Neumann, R. J. Phillips, S. C. Solomon, M. A. Wieczorek, and M. T. Zuber (2014), The formation of lunar mascon basins from impact to contemporary form, *J. Geophys. Res. Planets*, *119*, 2378–2397, doi:10.1002/2014JE004657.

Hartmann, W. K. (1980), Dropping stones in magma oceans: Effects of early lunar cratering, in *Proceedings of the Conference on the Lunar Highlands Crust*, edited by J. J. Papike and R. B. Merrill, pp. 155–171, Pergamon Press, New York.

Head, J. W., III, C. I. Fassett, S. J. Kadish, D. E. Smith, M. T. Zuber, G. A. Neumann, and E. Mazarico (2010), Global distribution of large lunar craters: Implications for resurfacing and impactor populations, *Science*, *329*, 1504–1507, doi:10.1126/science.1195050.

Henkel, H., T. C. Ekneligoda, and S. Aaro (2010), The extent of impact induced fracturing from gravity modeling of the Granby and Tvären simple craters, *Tectonophysics*, *485*, 290–305, doi:10.1016/j.tecto.2010.01.008.

Hörz, F., R. Grieve, G. Heiken, P. Spudis, and A. Binder (1991), Lunar surface processes, in *Lunar Sourcebook*, edited by G. H. Heiken, D. T. Vaniman, and B. M. French, pp. 61–121, Cambridge Univ. Press, New York.

Innes, M. J. S. (1961), The use of gravity methods to study the underground structure and impact energy of meteorite craters, *J. Geophys. Res.*, *66*, 2225–2239, doi:10.1029/JZ066i007p02225.

Konopliv, A. S., et al. (2014), High-resolution lunar gravity fields from the GRAIL Primary and Extended Missions, *Geophys. Res. Lett.*, *41*, 1452–1458, doi:10.1002/2013GL059066.

Main, I. G., T. Leonard, O. Papasouliotis, C. G. Hatton, and P. G. Meredith (1999), One slope or two? Detecting statistically significant breaks of slope in geophysical data, with application to fracture scaling relationships, *Geophys. Res. Lett.*, *26*, 2801–2804, doi:10.1029/1999GL005372.

Melosh, H. J. (1989), *Impact Cratering: A Geologic Process*, Oxford Univ. Press, New York.

Melosh, H. J., et al. (2013), The origin of lunar mascon basins, *Science*, *340*, 1552–1555, doi:10.1126/science.1235768.

Milbury, C., B. C. Johnson, H. J. Melosh, G. S. Collins, D. M. Blair, J. M. Soderblom, and M. T. Zuber (2015), The effect of pre-impact porosity on the gravity signature of lunar craters, *Lunar Planet. Sci.*, *46*, Abstract 1966.

Miljković, K., M. A. Wieczorek, G. S. Collins, M. Laneuville, G. A. Neumann, H. J. Melosh, S. C. Solomon, R. J. Phillips, D. E. Smith, and M. T. Zuber (2013), Asymmetric distribution of lunar impact basins caused by variations in target properties, *Science*, *342*, 724–726, doi:10.1126/science.1243224.

Minton, D. A., J. E. Richardson, and C. I. Fassett (2015), Re-examining the main asteroid belt as the primary source of ancient lunar craters, *Icarus*, *247*, 172–190, doi:10.1016/j.icarus.2014.10.018.

Navarre-Sitchler, A., and S. Brantley (2007), Basalt weathering across scales, *Earth Planet. Sci. Lett.*, *261*, 321–334, doi:10.1016/j.epsl.2007.07.010.

Phillips, R. J., C. J. Thomason, J. W. Head, J. M. Soderblom, F. Nimmo, J. Besserer, H. J. Melosh, C. Milbury, W. S. Kiefer, and M. T. Zuber (2015), Crater Bouguer anomalies probe South Pole-Aitken (SPA) basin structure, *Lunar Planet. Sci.*, *46*, Abstract 2897.

Pike, R. J. (1977), Size-dependence in the shape of fresh impact craters on the Moon, in *Impact and Explosion Cratering*, edited by D. J. Roddy, R. O. Pepin, and R. B. Merrill, pp. 489–509, Pergamon Press, New York.

Pike, R. J. (1988), Geomorphology of impact craters on Mercury, in *Mercury*, edited by F. Vilas, C. R. Chapman, and M. S. Matthews, pp. 65–273, Univ. of Arizona Press, Tucson.

Pilkington, M., and R. A. F. Grieve (1992), The geophysical signature of terrestrial impact craters, *Rev. Geophys.*, *30*, 161–181, doi:10.1029/92RG00192.

Pohl, J., D. Stöffler, H. Gall, and K. Ernstson (1977), The Ries impact crater, in *Impact and Explosion Cratering*, edited by D. J. Roddy, R. O. Pepin, and R. B. Merrill, pp. 343–404, Pergamon Press, New York.

Richardson, J. E. (2009), Cratering saturation and equilibrium: A new model looks at an old problem, *Icarus*, *204*, 697–715, doi:10.1016/j.icarus.2009.07.029.

Scott, E. R. D., and L. Wilson (2005), Meteoritic and other constraints on the internal structure of small asteroids, *Icarus*, *174*, 46–53, doi:10.1016/j.icarus.2004.10.014.

Smith, D. E., et al. (2010), The Lunar Orbiter Laser Altimeter investigation on the Lunar Reconnaissance Orbiter mission, *Space Sci. Rev.*, *150*, 209–241, doi:10.1007/s11214-009-9512-y.

Strom, R. G., R. Malhotra, Z.-Y. Xiao, T. Ito, F. Yoshida, and L. R. Ostrach (2015), The inner solar system cratering record and the evolution of impactor populations, *Res. Astron. Astrophys.*, *15*, 407–434, doi:10.1088/1674-4527/15/3/009.

Sugano, T., and K. Heki (2004), Isostasy of the Moon from high-resolution gravity and topography data: Implication for its thermal history, *Geophys. Res. Lett.*, *31*, L24703, doi:10.1029/2004GL022059.

Toksöz, M. F., A. M. Dainty, S. C. Solomon, and K. R. Anderson (1974), Structure of the Moon, *Rev. Geophys. Space Phys.*, *12*, 539–567, doi:10.1029/RG012i004p00539.

Warren, P. H., and K. L. Rasmussen (1987), Megaregolith insulation, internal temperatures, and bulk uranium content of the Moon, *J. Geophys. Res.*, *92*, 3453–3465, doi:10.1029/JB092iB05p03453.

Wieczorek, M. A., and R. J. Phillips (1999), Lunar multiring basins and the cratering process, *Icarus*, *139*, 246–259, doi:10.1006/icar.1999.6102.

Wieczorek, M. A., et al. (2013), The crust of the Moon as seen by GRAIL, *Science*, *339*, 671–675, doi:10.1126/science.1231530.

Zuber, M. T., et al. (2013), Gravity field of the Moon from the Gravity Recovery and Interior Laboratory (GRAIL) mission, *Science*, *339*, 668–671, doi:10.1126/science.1231507.